Giant vacuum-field Rabi splitting of intersubband transitions in multiple quantum wells

E. Dupont,* J. A. Gupta, and H. C. Liu
Institute for Microstructural Sciences, National Research Council, Ottawa, Ontario K1A 0R6, Canada
(Received 21 December 2006; published 17 May 2007)

A large, 42 meV, vacuum-field Rabi splitting was observed between the upper and lower intersubband polariton branches of a moderately *n*-doped GaAs-AlGaAs multiple quantum well sample. For this structure, the Rabi energy represents 17% of the bare intersubband resonance, a situation corresponding to the ultrastrong coupling regime between the photon and intersubband excitations. A different phenomenon is also demonstrated: the occurrence of a higher mode polariton. The large tunability of the intersubband absorption with carrier concentration may lead to new optoelectronic devices.

DOI: 10.1103/PhysRevB.75.205325 PACS number(s): 78.67.De, 42.50.Ct, 71.36.+c

I. INTRODUCTION

In 2003, two groups demonstrated a strong coupling regime between intersubband electronic transitions taking place in quantum wells (QWs) and confined photons in a resonator.[1,2] In these experiments, the vacuum-field Rabi frequency Ω_R was already significant: about 5% of the "natural" intersubband resonance ω_{12}. The occurrence of such a strong effect encouraged researchers to look for applications for the intersubband polaritons, such as quantum-well infrared photodetectors[2] (QWIPs) and modulators.[3] Several interesting research proposals based on intersubband polaritons were described, including tunable intersubband light-emitting devices.[4] More recently, the quantum properties of the intersubband polaritons were discussed by Ciutti *et al.*, particulary in the ultrastrong coupling regime.[5] In such a regime, Ω_R is a significant portion of the intersubband resonance ω_{12} and the ground state of the polaritonic system is very dependent on the cavity properties. When the cavity is perturbed in a nonadiabatic manner, fascinating quantum electrodynamic effects are predicted, such as the emission of correlated photon pairs that are artificially released, or "unbound," from the polariton vacuum state. Notably, Refs. 4 and 5 consider devices with very large vacuum Rabi energies, a regime which was not explored experimentally.

Recently, we have demonstrated Rabi frequencies of the order of 5% of the intersubband resonance in QWIP structures doped at 2×10^{10} cm^{-2}.[2] In the present paper, we show that, in similar structures, the vacuum Rabi frequency scales as the square root of the doping density, as predicted by the classical model.[6] In the highest-doped structure, we observe a vacuum Rabi splitting energy of 42 meV for an intersubband resonance at 123 meV. From the same structure, we report a strong absorption peak between the two polariton branches, on the low-energy side of the intersubband resonance. We show that this extra feature is related to the proximity of the $m=1$ excited mode of the low-quality factor and highly dispersive cavity. The high dispersion of this cavity is caused by the strong intersubband anomalous dispersion in the multiple-quantum-well (MQW) region. This additional peak can be explained by the same semiclassical model which describes the polariton branches, allowing us to identify this as a high-order mode polariton. This experiment shows that the absorption profile of an intersubband oscillator can be manipulated easily, and as a result, the device can be transformed into a broadband detector, a feature which could be useful in applications such as thermal imaging. According to Ref. 5, the effect of ultrastrong coupling is already non-negligible in our moderately doped QWIP; i.e., the polariton state cannot be simply described by a linear combination of photon and intersubband excitations.

II. DESCRIPTION OF THE SAMPLES AND EXPERIMENTS

The MQW structures of this study were designed as the core of a single-side surface plasmon waveguide similarly to those described in Ref. 2. The number of periods was adjusted in order to overlap the intersubband resonance with the resonant mode of the waveguide at Brewster incidence on the cleaved facet. The two samples discussed in this article are labeled wafer L and wafer M, and were grown by molecular-beam epitaxy on 3 in. (001) GaAs semi-insulating substrates. They were grown one after the other. They consist of a 160-repeat ($N_{QW}=160$) MQW structure embedded between a 0.4-μm-thick n^+ GaAs top contact layer and 0.8 μm n^+ GaAs bottom layer with a Si-doping level of 2×10^{18} cm^{-3}. Nominally, the period of the MQW consists of a 75 Å GaAs quantum well and a 290 Å $Al_{0.25}Ga_{0.75}As$ barrier. The confinement energy of the first excited state e_2 is 66 meV which makes the intersubband resonance $e_1\rightarrow e_2$ strongly bound to bound. The wells are center delta doped with Si to 2×10 cm^{-2} (wafer L, for low doping) or 2×10^{11} cm^{-2} (wafer M, for moderate doping). From x-ray-diffraction measurements, the barrier and well thicknesses were found to be 290.4 and 74.6 Å for wafer L; 286.8 and 73.6 Å for wafer M. The Al content in the barrier is 0.2565 for both structures. From secondary-ion-mass spectrometry measurements, the Si doping in the contacts was found to be 2.24×10^{18} cm^{-3} and in the QWs the dopant concentration is very close to the nominal value. The similarity of the structural parameters of the two wafers (except for the delta-doping level) suggests that the two cavities are identical.

Initially, the depolarization-shifted intersubband resonances were measured at 80 K with a Fourier transform infrared spectrometer, either by measuring the transmission of *P*-polarized infrared light at Brewster incidence for wafer M or by measuring the ratio between the transmission of *P*- and *S*-polarized lights through a zigzag waveguide with 45° fac-

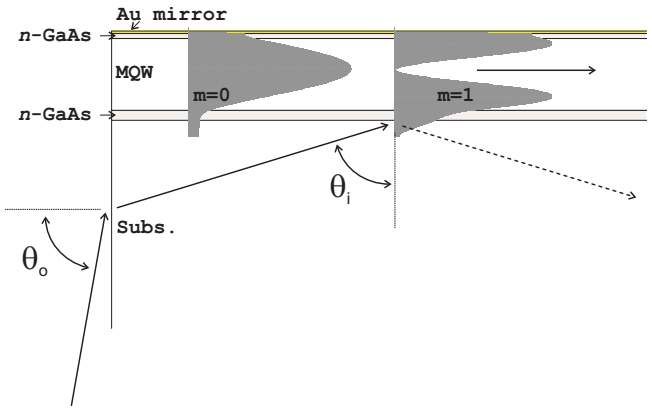

FIG. 1. (Color online) Schematic of the prismlike coupling technique for coupling infrared light into the QWIP waveguide. As an example, two TM modes at 860 cm^{-1} are displayed (as the modulus squared of the transverse magnetic field) assuming an empty cavity, i.e., with undoped QWs. The displayed fundamental mode $m=0$ is excited for an internal incidence $\theta_i=72°$; the excited mode $m=1$ would appear for $\theta_i=61.5°$. The modes exhibit significant leakage into the substrate for this low-quality factor resonator.

ets for the low doped wafer L. Secondly, a 25/2000 Å Ti/Au mirror was deposited on the epilayers and $(2\times n\times d)$-long samples were cleaved, where n is the index of refraction of GaAs and d the sample thickness. With these parallelograms, the infrared beam bounces once on the epilayers for Brewster incidence on the cleaved facet. At a particular wavelength and internal incidence, the incoming beam can excite a slab waveguide mode and can subsequently be absorbed in the contacts and in the MQW. Similar results were obtained at ambient temperature (not shown here), but the effects described in this paper are stronger at low temperature due to a smaller intersubband broadening.

Figure 1 shows the coupling scheme between the incoming infrared beam and the single-side surface plasmon waveguide which is formed by the mirror, the top contact, the MQW, and the bottom contact. Two examples of TM-mode profiles at 860 cm^{-1} of an empty cavity, i.e., with undoped QWs, are also represented. The fundamental mode $m=0$ would be excited for an internal incidence $\theta_i=72°$; the next one, $m=1$ for $\theta_i=61.5°$. These modes leak significantly into the substrate, especially the $m>0$ modes, due to the low quality factor (Q_{cav}) of the cavity. In this example, Q_{cav} is 16.4 at 72° internal incidence and only 9.5 at 61.5°. The samples were mounted inside a liquid-nitrogen dewar, which was mounted on a rotating stage. Transmission of P- and S-polarized lights through the parallelogram was measured and their ratio calculated. We did not observe special features or resonances with the S-polarized signal. These spectroscopic measurements are summarized in Figs. 2 and 3, respectively, for wafers L and M. From the Brewster transmittance and the 45° zigzag measurements, we derived the product between the oscillator strength f_{12} and free carrier concentration N_s. We get $N_s f_{12}=1.68\times 10^{10}$ and 1.92×10^{11} cm^{-2} for wafer L and wafer M, respectively. Theoretically, when taking into account nonparabolicity, the oscillator strength should be 0.84.[7] The same fitting procedure leads to the mobility of the contact: 4240 $cm^2\ V^{-1}\ s^{-1}$. Interest-

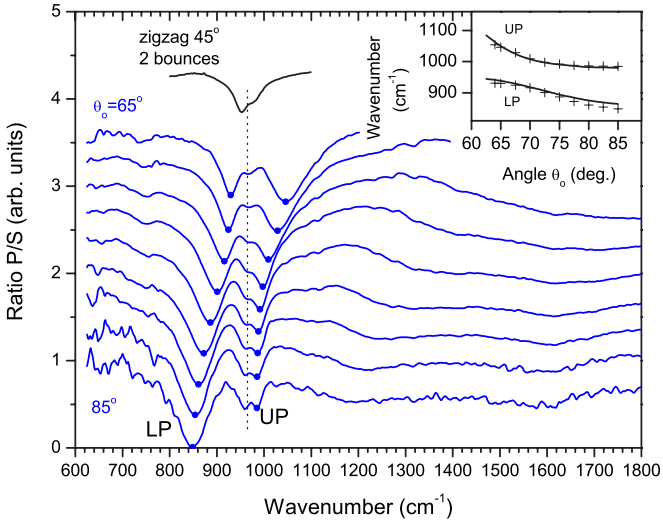

FIG. 2. (Color online) Normalized ratios between P-polarized and S-polarized transmittance at 80 K of the waveguide sample made from wafer L for different external angles θ_o. For clarity, the spectra are shifted relative to each other by 0.35. The frequency resolution is 4 cm^{-1}. The polariton resonances have been highlighted by a dot. The top curve represents the P/S ratio for a two-bounce 45° zigzag waveguide. The vertical dashed line represents the centroid position of the absorption peak. The inset plot shows the resonance positions of the upper polariton (UP) and lower polariton (LP) versus the external angle; the crosses (+) are experimental points and the solid line represents the theoretical calculation based on a semiclassical model.

ingly, the full width at half maximum $\Delta\omega_{12}$ of the absorption peak on wafer L ($\sim$63 cm^{-1}) is similar to that of wafer M ($\sim$55 cm^{-1}) which is ten times more doped. This explains why the absorption could barely be observed in the Brewster geometry on wafer L. From the topmost spectrum of Fig. 2,

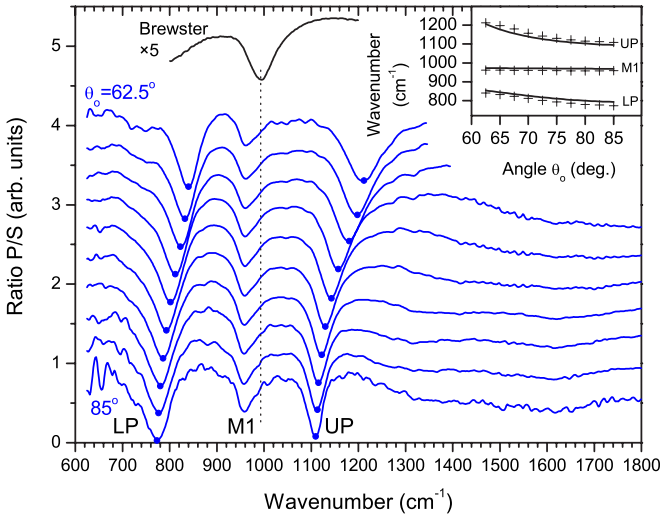

FIG. 3. (Color online) Summary plot for wafer M. The caption is similar to that of Fig. 2. Additionally, the inset plot shows the experimental (+) and predicted (solid line) frequencies of the higher mode (M1) polariton. The top curve is the P transmission at Brewster angle with a fivefold expansion of the vertical scale.

the absorption peak appears to consist of two Lorentzians centered at 950 and 965 cm^{-1} (the latter being more intense), suggesting the occurrence of inhomogeneous broadening in wafer L.

III. INTERPRETATION OF THE REFLECTIVITY SPECTRA

The minimum separation between the lower and upper polariton branches is about 93 cm^{-1} at $\theta_o \sim 70°$ for wafer L and 336 cm^{-1} (42 meV; $\Omega_R = 21$ meV) at $\theta_o \sim 80°$ for wafer M. The anticrossing for wafer L was expected to occur at an outside angle θ_o 10° smaller than that of wafer M since the intersubband frequency is 28 cm^{-1} smaller on the low-doped structure. The ratio between the vacuum Rabi splitting of the two structures, 336 cm^{-1}/93 cm^{-1} =3.61, is consistent with the square root dependance of vacuum-Rabi energy on the number of oscillators, i.e., $\sqrt{1.92\times10^{11}\ cm^{-2}/1.68\times10^{10}\ cm^{-2}}=3.38$. The plots in the insets of Figs. 2 and 3 represent the experimental frequencies of the upper and lower polaritons as a function of the outside angle θ_o and the theoretical results of these resonances. One can see that the agreement between the experimental results and theory is very satisfactory. However, the recorded minimum splitting is 5% higher than the theoretical value on wafer L and 10% on wafer M. The origin of these deviations are under investigation.

Qualitatively, the full width at half maximum of the polariton branches on both samples behaves normally. As the branches get closer to the bare intersubband frequency, the broadening of the polariton resonances decreases since the quality factor of the intersubband oscillator ($Q_{ISB} \sim 20$) is higher than the photon mode [$Q_{cav} \sim 16.5(12)$ at 860(1130) cm^{-1}]. This is particulary clear in Figs. 2 and 3 on the lower polariton (LP) [upper polariton (UP)] branch of wafer L (wafer M). The mixing between the electroniclike and photonlike behaviors of a polariton is evident at the UP branch of wafer M and large external angles. This branch at 1110 cm^{-1} is narrow (~40 cm^{-1}), even though it is far detuned from ω_{12}. At slightly longer wavelength, around 1050 cm^{-1}, the broadening of UP polariton of wafer L, which is mainly photonlike, is significantly larger, about ~80 cm^{-1}.[8] A similar comparison, which indicates the mixed photonlike and electroniclike nature of the polariton, can be made between the LP polariton branches of the two samples. On the reflectivity spectrum of wafer L at $\theta_o = 85°$, the LP branch at ~850 cm^{-1} is mainly photonlike and broad (~80 cm^{-1}), whereas the LP polariton of wafer M at $\theta_o = 62.5°$ is narrow (~50 cm^{-1}), even though it is also centered at ~850 cm^{-1}.

Quantitatively and within the semiclassical model used in this work, an exact fitting of the spectra of wafer M, more specifically the broadening of the polariton resonances, could not be obtained. We used a Lorentzian intersubband dispersion in the dielectric function ϵ_{zz} of the QWs. As shown in Fig. 4, we cannot simulate the narrow UP polariton at large external angles. In Fig. 3, this resonance appears narrower (~33 cm^{-1} at $\theta_o = 85°$) than the bare intersubband oscillator (55 cm^{-1}), while the Q_{cav} of an empty cavity corresponds to

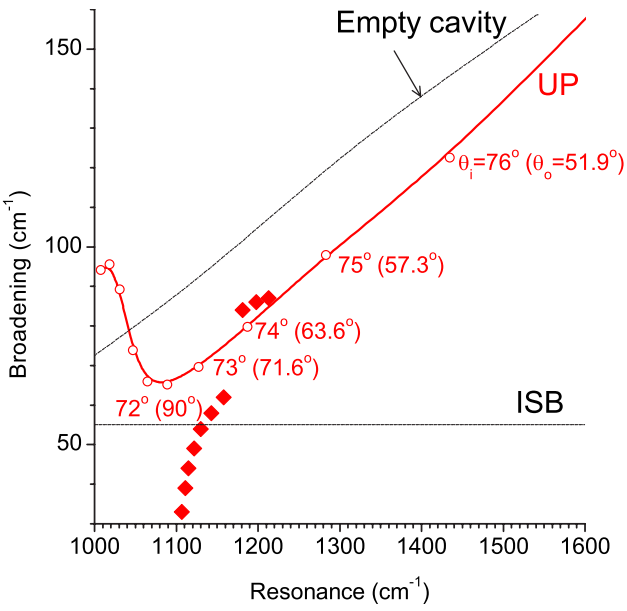

FIG. 4. (Color online) Full width at half maximum of the UP branch vs wave number of the resonance. The thick red solid line corresponds to the theoretical estimation based on a semiclassical model and the squares correspond to the experimental points. The internal and external angles used for the polariton simulation are indicated in the vicinity of the solid line. The horizontal (slanted) dash dotted line represents the broadening of the bare intersubband resonance (empty cavity $m=0$ mode resonance).

a large broadening ⩾90 cm^{-1}. This effect was also observed at ambient temperature. The narrowing of UP polariton branch when the frequency of the empty cavity $m=0$ mode approaches the intersubband frequency suggests that the electronic excitation is strongly inhomogeneous.[9] We have seen that the intersubband transitions are inhomogeneous in the low-doped sample, wafer L. Therefore, it is not surprising to observe the inhomogeneous broadening on wafer M. The narrowing effect can be clearly observed if the Rabi energy is significantly larger than both excitation broadenings, which is the case with wafer M. The effect of narrowing of the polariton branches was well explained theoretically and demonstrated experimentally in excitonic systems.[9] Following the model of Ref. 9, we estimate that the homogeneous (inhomogeneous) broadening is 20 (40) cm^{-1} or less (more). We also find that LP polariton is broader than expected at large external angles, i.e., at long wavelength, which could be related to an underestimated loss in the contacts, in the mirror, and most likely, in the MQW due to free carrier absorption in the confinement direction.[10]

The polariton tuning curves of wafer L is very similar to what was reported in Ref. 2. As already explained,[2] the observed central dip between the two polariton branches is associated with the low Q_{cav} of the cavity and the narrow intersubband resonance. The low Q_{cav} allows a significant tunneling of the light through the bottom contact which, in turn, probes the intersubband transition. At the intersubband resonance frequency, the cavity is in the strongly damped regime, i.e., $\alpha_{ISB} d_{MQW} > -\ln(\sqrt{R_1})$, where α_{ISB} is the average intersubband absorption coefficient in the MQW, d_{MQW} the

thickness of the MQW, and R_1 the reflectivity of the bottom n contact. In this situation, the absorption of the device converges toward $(1-R_1) \gg 0$.[11] Outside the intersubband resonance, the absorption is smaller, which puts the cavity in the moderately damped regime $[\alpha_{\mathrm{ISB}} d_{\mathrm{MQW}} < -\ln(\sqrt{R_1})]$, while the light is much less confined in the MQW due to the strong intersubband dispersion associated with the real part of the intersubband susceptibility. Both effects induce a reduction of the total absorption, below $(1-R_1)$. As a result, the reflectivity of the device around the intersubband frequency illustrates the intersubband absorption. A quantitative treatment of the central peak is given in Ref. 12. In this paper, the authors explain that $(N_{\mathrm{QW}}-1)$-fold degenerate radiative intersubband polariton modes at $\hbar\omega_{12}$ are usually "dark" modes unless special conditions on the cavity are fulfilled.

However, the polariton tuning curves of wafer M look different from those of wafer L between the two main branches, as if the behavior lies in another regime in the moderately doped wafer. One observes a peak between 958 and 962 cm^{-1}, called M1 in Fig. 3, which is fairly detuned from the intersubband resonance $\omega_{12}=993\ \mathrm{cm}^{-1}$. A slight redshift, linewidth narrowing, and increase in the absorption intensity are observed when the outside angle increases. Additionally, this peak does not show the usual Lorentzian profile, but looks triangular with a slightly more pronounced tail on its high-energy side.

Simple calculations indicate that the feature M1 is related to the occurrence of a higher mode polariton. Using the effective medium approach in the MQW,[13] we calculated the phase shift of a TM-polarized light during the propagation along a double pass through the MQW, as well as the phase shift of the reflection coefficients of the bottom and top mirrors ψ_1 and ψ_2. For simplicity, we used a Lorentzian model for the intersubband susceptibility as if the transition were homogeneously broadened. Basically, our calculations are numerical applications of the semiclassical model developed by Zhu *et al.*[6] Simulations do not predict sharp resonances or strongly angle-dependent features in the S polarization. Provided the cavity is not strongly damped, cavity resonances occur when the sum of these three phases $\Delta\phi$ is a multiple of 2π,

$$\Delta\phi = 2\Re(k_{z,\mathrm{MQW}}) d_{\mathrm{MQW}} + \psi_1 + \psi_2 = 2m\pi \quad (m = 0,1,2,\ldots), \tag{1}$$

where $k_{z,\mathrm{MQW}}$ is the projection of wave vector in the MQW on the growth direction. The phase calculation is summarized in Fig. 5(a). The discontinuity of the phase for a high doping $5N_s$ is simply related to the phase of reflection coefficient of the bottom mirror which is calculated between $\pm\pi$ modulo 2π. An empirical model was used for the dispersion of gold.[14] The finesse of the cavity is calculated for an empty cavity $(N_s=0)$ is represented as gray horizontal regions around $m=0,1,2$. For $m=0$ and $m=1$, the finesse is larger at longer wavelength due to the enhanced reflectivity of the bottom mirror.[15] Of course, the less confined $m=1$ modes have smaller finesse than the fundamental modes. As expected, the $m=2$ modes are leaky and are not very resonant. The intersubband cavity loss spectra are plotted in Fig. 5(b).

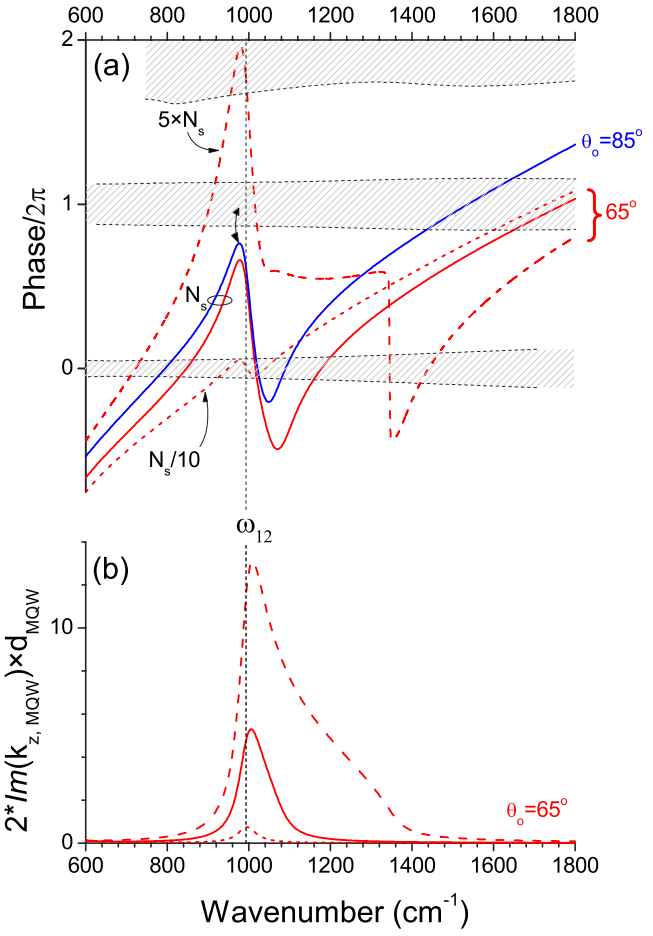

FIG. 5. (Color online) (a) Calculated phase versus wave number for TM-polarized light during a double pass in the cavity for different external angles θ_o and doping concentrations. The parameters used for the simulations are $N_s f_{12}=1.92\times10^{11}\ \mathrm{cm}^{-2}$, $\omega_{12}=993\ \mathrm{cm}^{-1}$, $\Delta\omega_{12}=55\ \mathrm{cm}^{-1}$, n-contact layers doped to $2.24\times10^{18}\ \mathrm{cm}^{-3}$, and mobility of $4240\ \mathrm{cm}^2\ \mathrm{V}^{-1}\ \mathrm{s}^{-1}$. The gray horizontal regions represent the finesse of the cavity resonances. The vertical dashed line shows the position of the intersubband resonance. The double black arrow shows the proximity of the excitation of an $m=1$ polariton. (b) Spectra of the cavity losses due to the intersubband transitions, i.e., the product of the imaginary part of the wave vector inside the MQW with the thickness of the MQW at an external incident angle of $\theta_o=65°$ and for three different doping levels $N_s/10$, N_s, and $5N_s$.

The phase spectra in Fig. 5(a) cross the $m=0$ resonance at the polariton frequencies and near the intersubband resonance, this latter being strongly damped. Between the polariton branches, the spectra for N_s and $N_s/10$ cross the $m=0$ cavity resonance at a frequency slightly higher than ω_{12}; in other words, the bare cavity mode is blueshifted, as already discussed in Ref. 5. For a N_s doping and for frequencies close to $\omega_{12}-\Delta\omega_{12}/2$, the intersubband dispersion is high enough to move the cavity close to the next $m=1$ mode. Because the finesse of our resonator is small, the coupling to the $m=1$ mode is tolerated even though the phase does not reach 2π. As seen in Fig. 5(b), the MQW loss is strongly varying at the frequencies $\omega \sim \omega_{12}-\Delta\omega_{12}/2$, which in turn,

induces a slight redshift of the observed resonance in reflectivity compared to the frequency at which the expression $|\Delta\phi - 2\pi|$ is minimized. Additionally, the strong intersubband absorption increases the absorption of the device on the high-energy side of the $m=1$ resonance, which makes the resonant peak slightly asymmetric. Our simulation predicts that the central peak M1 should be at $\sim 970\ \mathrm{cm}^{-1}$, as opposed to $\sim 959\ \mathrm{cm}^{-1}$ in the experiment. This slight discrepancy, which is under investigation, does not invalidate the general interpretation of the excitation of a higher mode polariton, an interpretation which is also supported in Ref. 12.

IV. CONCLUSION

We have demonstrated a vacuum Rabi frequency of the order of the bare intersubband frequency in a moderately doped MQW structure. At 17% of the intersubband frequency, the cavity is expected to experience some effects due to the ultrastrong coupling regime. In such a regime, the proportions of the electronlike and photonlike characteristics of the polaritons are theoretically complex. Absorption saturation experiments of the polaritons on both samples could help to determine the photon-matter nature of these mixed modes and to confirm the role of ultrastrong coupling regime. Additionally, we have demonstrated the square-root dependence of the vacuum Rabi energy versus the number of oscillators, the mixed photonlike and electronlike nature of the polaritons, the occurrence of a higher-mode polariton, and finally, the inhomogeneous broadening of the intersubband excitations. By further increasing the doping level, one could try to observe the interaction between the LP polariton and two-phonon excitation, a hybridized mode which could lead to interesting physics in a new regime.

*Electronic address: emmanuel.dupont@nrc-cnrc.gc.ca

[1] D. Dini, R. Köhler, A. Tredicucci, G. Biasiol, and L. Sorba, Phys. Rev. Lett. **90**, 116401 (2003).

[2] E. Dupont, H. C. Liu, A. J. SpringThorpe, W. Lai, and M. Extavour, Phys. Rev. B **68**, 245320 (2003).

[3] A. A. Anappara, A. Tredicucci, G. Biasiol, and L. Sorba, Appl. Phys. Lett. **87**, 051105 (2005).

[4] R. Colombelli, C. Ciuti, Y. Chassagneux, and C. Sirtori, Semicond. Sci. Technol. **20**, 985 (2005).

[5] C. Ciuti, G. Bastard, and I. Carusotto, Phys. Rev. B **72**, 115303 (2005).

[6] Y. Zhu, D. J. Gauthier, S. E. Morin, Q. Wu, H. J. Carmichael, and T. W. Mossberg, Phys. Rev. Lett. **64**, 2499 (1990).

[7] C. Sirtori, F. Capasso, J. Faist, and S. Scandolo, Phys. Rev. B **50**, 8663 (1994).

[8] The broadening of the UP polariton would be even larger at 1120 cm^{-1} (for $\theta_o < 65°$) since the reflectivity of the bottom mirror decreases with frequency.

[9] R. Houdré, R. P. Stanley, and M. Ilegems, Phys. Rev. A **53**, 2711 (1996).

[10] The perpendicular permittivity of the QW used for the simulations did not include the free carrier susceptibility in the growth direction which can be derived by second-order perturbation theory. For instance, a free carrier absorption calculation is described in I. Vurgaftman and J. R. Meyer, Phys. Rev. B **60**, 14294 (1999).

[11] M. S. Ünlü and S. Strite, J. Appl. Phys. **78**, 607 (1995).

[12] M. Załużny and W. Zietkowski (unpublished).

[13] M. Załużny and C. Nalewajko, Phys. Rev. B **59**, 13043 (1999).

[14] M. A. Ordal, R. J. Bell, R. W. Alexander, L. L. Long, and M. R. Querry, Appl. Opt. **26**, 744 (1987).

[15] For instance, for an internal angle $\theta_i = 73°$, the reflectivity of the bottom mirror is 94% at 600 cm^{-1} and drops to 13% at 1800 cm^{-1}. The plasma frequency of the n^+ GaAs is 525 cm^{-1}.